INVESTIGATION OF THE RELATIONSHIP BETWEEN VEGETATION INDEXES AND NORMALIZED DIFFERENCE VEGETATION INDEX IN COTTON FIELDS

S. Kılıçaslan*[,1], R. Ekinci[2] and M. C. Arslanoğlu[3]

[1]Department of Field Crops, Institute of Science and Technology,Dicle University, 21280, Diyarbakir/Turkiye,
[2]Department of Field Crops, Faculty of Agriculture,Dicle University, 21280, Diyarbakir/Turkiye,
[3]Department of Computer Engineering, Faculty of Engineering and Architecture, Batman University, Batman/ Turkiye

*Corresponding author email:3serkankilicaslan@hotmail.com

[1](Orcid ID: 0000-0002-5595-2338), [2](Orcid ID: 0000-0003-4165-6631), [3](Orcid ID: 0000-0001-5152-569X),

ABSTRACT

This study aimed to evaluate the relationship of 12 vegetation indices (VIs) derived from satellite imagery with field-measured Normalized Difference Vegetation Index (NDVI) in cotton, with particular emphasis on measurement agreement, phenology-dependent variation, and shared versus complementary information content. In this context, Atmospherically Resistant Vegetation Index (ARVI), Green Atmospherically Resistant Vegetation Index (GARI), Enhanced Vegetation Index 2 (EVI 2), Modified Triangular Vegetation Index 2 (MTVI2), Modified Normalized Difference Vegetation Index (MNDVI), Moisture Stress Index (MSI), Normalized Difference Moisture Index (NDMI), Ratio Drought Index (RDI), Modified Red-Edge Normalized Difference Vegetation Index (MRENDVI), Structure Insensitive Pigment Index (SIPI), Soil-Adjusted Vegetation Index (SAVI) and Modified Soil-Adjusted Vegetation Index (MSAVI) derived from Sentinel-2 imagery were compared with NDVI measurements obtained using a GreenSeeker handheld sensor across different phenological stages. Relationships were examined using regression analysis, Bland–Altman analysis, and principal component analysis (PCA). Models incorporating phenological stage effects showed that the index–NDVI relationships were generally strong at the seasonal scale (R^2 = 0.848–0.867), but varied according to both index type and phenological stage. Stage-wise analyses further indicated that the strongest relationships were consistently observed in the early season, whereas explanatory power declined during the mid- and especially late-season. MTVI2, MSAVI, ARVI, and GARI exhibited patterns more similar to NDVI in tracking canopy development, whereas NDMI, MSI, RDI, MRENDVI, SIPI, and partly EVI2 reflected distinct sensitivities related to water status, pigment composition, and physiological change. These findings suggest that the tested indices should not be interpreted in terms of single-index superiority, but rather in terms of overlapping and complementary information under different phenological and biophysical conditions. Overall, for vegetation monitoring in cotton, a multi-index framework selected according to phenological stage and monitoring objective appears more appropriate than a single-index approach.

Keywords: Cotton, NDVI, Vegetation Indexes, Sentinel-2, GreenSeeker

https://doi.org/10.36899/JAPS.2026.5.0107 Published first online June, 07, 2026

INTRODUCTION

Crop growth monitoring is a core component of precision agriculture because it supports key management decisions, including irrigation, fertilization, stress assessment, yield estimation, and harvest planning (Sishodia *et al.*, 2020). Recent advances in satellite systems and unmanned aerial vehicles have enabled vegetation monitoring over large areas at high spatial and temporal resolution, while cloud-based platforms and data-driven approaches have become increasingly important for processing these data (Defourny *et al.*, 2019; Maimaitijiang *et al.*, 2020; Sishodia *et al.,* 2020). Despite these developments, the interpretation of spectral information in agricultural monitoring still relies largely on vegetation indices (VIs).

Recent reviews have shown that VIs remain central to precision agriculture applications and that, although the Normalized Difference Vegetation Index (NDVI) is still the most widely used reference index, alternative indices may perform better under specific conditions (Radočaj *et al.*, 2023; Vidican *et al.,* 2023). At the same time, index selection is increasingly recognized as context-dependent, varying with the intended application, environmental conditions, and crop phenological stage (Zeng *et al.,* 2022; Vidican *et al.,* 2023). Conventional field observations and in situ measurements are labor-intensive, time-consuming, and spatially limited, which restricts their usefulness for continuous monitoring over large areas (Defourny *et al.,* 2019; Sishodia *et al.,* 2020). By contrast, in crops such as cotton (*Gossypium hirsutum* L.), which exhibit rapid growth and require timely management decisions, satellite- and unmanned aerial vehicle (UAV)-based approaches are being used increasingly, and variables such as crop coefficient, leaf area index, and plant height have been estimated successfully from remote sensing data (Kaplan *et al.,* 2023; Yang *et al.,* 2024).

NDVI is one of the most widely used indicators of vegetation development because it captures the contrast between chlorophyll absorption in the red band and internal leaf scattering in the near-infrared (NIR) region (Huang *et al.,* 2021). It is therefore commonly used as a benchmark in precision agriculture studies (Radočaj *et al.,* 2023). However, NDVI has well-documented limitations, including sensitivity to atmospheric effects, soil background, and saturation under high leaf area conditions (Rondeaux *et al*., 1996; Huang *et al.,* 2021). In cotton, rapid canopy development, variable soil reflectance, and increasing mixed-pixel effects during the late season may make these limitations more pronounced across phenological stages (Kaplan and Rozenstein, 2021; Wang *et al.,* 2023).

Remote sensing studies in cotton have mostly focused on the relationships between one index, or a limited number of indices, and specific target variables, particularly water stress, leaf area index, plant height, growth monitoring, and boll opening (Kaplan *et al.,* 2023; Wang *et al.,* 2023; Gu *et al.,* 2024). Although these studies are informative for specific applications, they provide limited insight into how different indices behave relative to NDVI, under which conditions they exhibit systematic differences, and how these relationships vary across phenological stages. In particular, phenology-sensitive studies that jointly compare a broad set of indices with field-derived NDVI in terms of relationship strength, agreement, and shared variation structure remain limited in the cotton literature (Zeng *et al.,* 2022; Tian *et al.,* 2023). There is therefore a clear need for comparative analyses that systematically identify the extent to which different VIs provides overlapping or complementary information relative to NDVI in cotton.

To address this gap, the present study compares 12 vegetation indices derived from satellite imagery against field-measured NDVI in cotton within a phenology-sensitive framework. The indices are evaluated not only in terms of correlation, but also with respect to linear association, agreement between measurements, systematic differences, and shared versus divergent variation structure within a unified analytical framework. This approach enables indices that closely track NDVI to be distinguished from those that may provide complementary information beyond it. Accordingly, the objectives of this study are to: (i) assess the strength of the relationship and the level of agreement between 12 vegetation indices and field-derived NDVI, (ii) determine how these relationships change across phenological stages, and (iii) examine whether the indices exhibit patterns that converge with or diverge from NDVI. Rather than testing the direct biophysical superiority of any single index, this study aims to identify patterns of similarity, divergence, and complementarity relative to NDVI.

MATERIALS AND METHODS

Study Area: The study area is located within the Upper Mesopotamian Basin, one of the major agricultural production regions of Türkiye (36.0°–42.0° N and 26.0°–45.0° E). The Mardin Plain is among the most favorable cotton-growing areas in the country owing to its hot semi-arid steppe climate and its deep, clay loam, irrigable soils. With the expansion of irrigation infrastructure and the increasing prevalence of double-cropping systems, cotton has assumed a strategic position within the province's production pattern and has become an important source of agricultural income for the regional population. The research was conducted in 27 cotton-planted fields located in 8 villages within the Artuklu and Kızıltepe districts of Mardin Province (Figure 1). According to the reference values of Güçdemir (2008) soil analyses based on samples collected from the study fields classified the soils as clay loam in texture, highly calcareous, non-saline or very slightly saline, slightly alkaline or neutral in reaction, low in organic matter, low to moderate in phosphorus content, and sufficient in potassium content (Table 1).

Table 1. Positional information of sampling points and some physical and chemical soil properties

No	Coordinates (x: y)	Saturation (%)	EC	pH	Lime %	Organic Matter (%)	Phosphorus	Potassium
S01	40.856; 37.139	64,90- Clay-Loam	0,89-Non-saline	7,81-Slightly Alkaline	23,9-Highly calcareous	1.59-Low	4,12- Low	148.4-Sufficient
S02	40.860; 37.138	58,30- Clay-Loam	0.79-Non-saline	7,77-Slightly Alkaline	26,8-Highly calcareous	1.56-Low	4.64- Low	148.3-Sufficient

S03	40.878; 37.142	63,80-Clay-Loam	0.98-Non-saline	7,64-Slightly Alkaline	27,8-Highly calcareous	1.61-Low	4.81- Low	157.6-Sufficient
S04	40.866; 37.136	63,80-Clay-Loam	1,09-Non-saline	7,65-Slightly Alkaline	22,3-Highly calcareous	1.53-Low	5.49- Low	169.8-Sufficient
S05	40.865; 37.134	64,90-Clay-Loam	1,42-Non-saline	7.52-Neutral	22,6-Highly calcareous	1.73-Low	7.21-Medium	179.1-Sufficient
S06	40.853; 37.129	61,60-Clay-Loam	0.86-Non-saline	7,63-Slightly Alkaline	22,7-Highly calcareous	1.70-Low	6.01- Low	159.9-Sufficient
S07	40.877; 37.157	63,80-Clay-Loam	0.85-Non-saline	7.69-Slightly Alkaline	22,0-Highly calcareous	1.82-Low	5.38- Low	202.3-Sufficient
S08	40.843; 37.152	58,96-Clay-Loam	1,07-Non-saline	7,83-Slightly Alkaline	22,9-Highly calcareous	1.90-Low	5.55- Low	193.6-Sufficient
S09	40.846; 37.157	64,90-Clay-Loam	1,34-Non-saline	7,68-Slightly Alkaline	23,4-Highly calcareous	1.85-Low	3.95- Low	226.6-Sufficient
S10	40.836; 37.128	62,04-Clay-Loam	0.89-Non-saline	7.79-Slightly Alkaline	22,3-Highly calcareous	1.79-Low	4.18- Low	154.1-Sufficient
S11	40.834; 37.128	67,10-Clay-Loam	1,04-Non-saline	7,84-Slightly Alkaline	24,6-Highly calcareous	1.76-Low	4.35- Low	160.8-Sufficient
S12	40.598; 37.119	61,60-Clay-Loam	1,47-Non-saline	7,68-Slightly Alkaline	20,6-Highly calcareous	1.87-Low	4.86- Low	187.7-Sufficient
S13	40.593; 37.124	61,16-Clay-Loam	1,32-Non-saline	7,77-Slightly Alkaline	20,8-Highly calcareous	1.93-Low	5.38- Low	194.0-Sufficient
S14	40.600; 37.114	58,08-Clay-Loam	1,13-Non-saline	7,73-Slightly Alkaline	21,1-Highly calcareous	1.85-Low	6.35-Medium	196.6-Sufficient
S15	40.611; 37.100	59,18-Clay-Loam	1,23-Non-saline	7,65-Slightly Alkaline	21,6-Highly calcareous	1.82-Low	6.07-Medium	216.8-Sufficient
S16	40.596; 37.101	63,80-Clay-Loam	2,86-Very slightly salty	7.35-Neutral	21,9-Highly calcareous	1.70-Low	7.73-Medium	228.8-Sufficient
S17	40.583; 37.094	55,00-Clay-Loam	0.75-Non-saline	7,82-Slightly Alkaline	22,2-Highly calcareous	1.76-Low	8.01-Medium	200.8-Sufficient
S18	40.578; 37.097	59,40-Clay-Loam	1,27-Non-saline	7.79-Slightly Alkaline	22,5-Highly calcareous	1.87-Low	6.12-Medium	166.3-Sufficient
S19	40.597; 37.109	57,20-Clay-Loam	1,15-Non-saline	7,80-Slightly Alkaline	22,6-Highly calcareous	1.79-Low	4.81- Low	182.5-Sufficient
S20	40.591; 37.067	60,50-Clay-Loam	2,70-Very Lightly	7,55-Slightly Alkaline	21,6-Highly calcareous	1.61-Low	3.78- Low	161.5-Sufficient

			Salty						
S21	40.590; 37.075	60,94-Clay-Loam	0.88-Non-saline	7,81-Slightly Alkaline	21,3-Highly calcareous	1.59-Low	4.12- Low	154.1-Sufficient
S22	40.531; 37.108	64,90-Clay-Loam	0.95-Non-saline	7,78-Slightly Alkaline	21,6-Highly calcareous	1.64-Low	3.66- Low	187.9-Sufficient
S23	40.538; 37.113	57,20-Clay-Loam	0.65-Non-saline	7,84-Slightly Alkaline	21,9-Highly calcareous	1.56-Low	3.95- Low	205.5-Sufficient
S24	40.565; 37.112	62,04-Clay-Loam	0.88-Non-saline	7,85-Slightly Alkaline	23,4-Highly calcareous	1.53-Low	4.46- Low	214.7-Sufficient
S25	40.549; 37.114	58,96-Clay-Loam	1,34-Non-saline	7,64-Slightly Alkaline	23,1-Highly calc***areous	1.59-Low	4.06- Low	226.6-Sufficient
S26	40.531; 37.072	57,20-Clay-Loam	1,05-Non-saline	7,74-Slightly Alkaline	23,6-Highly calcareous	1.70-Low	4.14- Low	215.7-Sufficient
S27	40.528; 37.073	57,20-Clay-Loam	0.83-Non-saline	7,72-Slightly Alkaline	24,1-Highly calcareous	1.67-Low	4.29- Low	211.1-Sufficient

Reference values source: (Güçdemir, 2008) Agriculture Handbook TÜGEM Ankara 2008

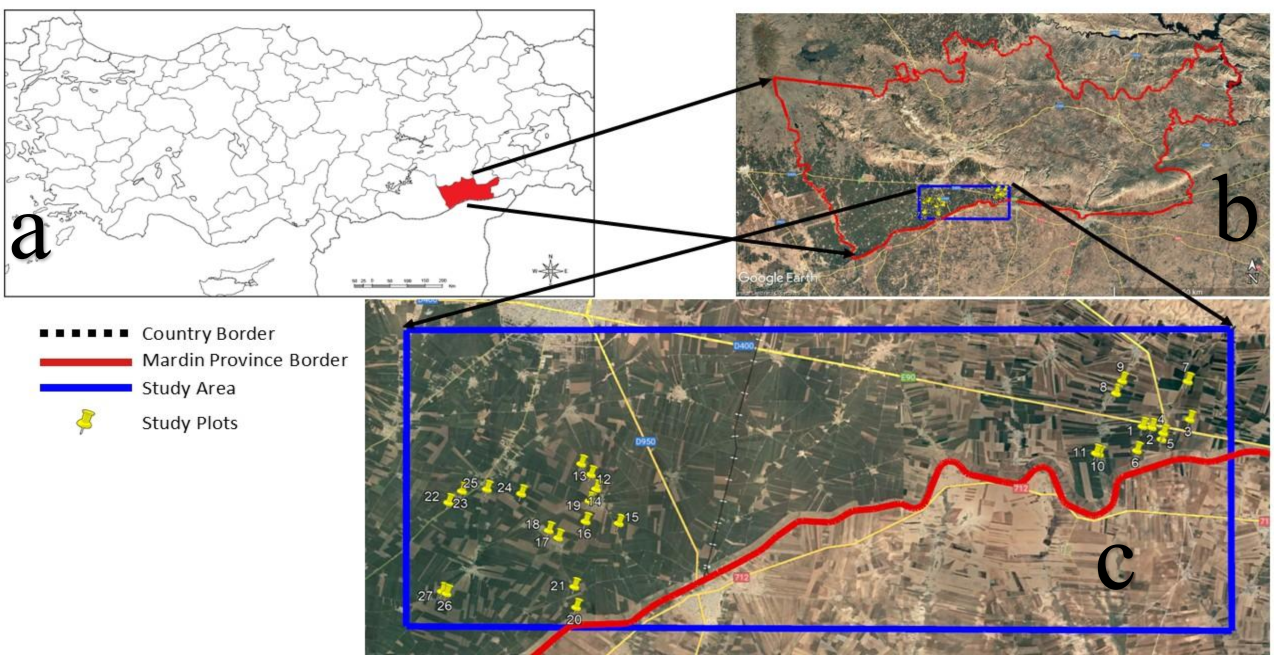

Figure 1. Study Area: (a) Country borders (b) Mardin province border c) study area region

In the Mardin Plain, 49% of the annual precipitation occurs in winter, 37% in spring, 13% in autumn, and only 0.9% in summer (Bahçeci and Aydın, 2008). No rainfall was recorded in the region during the June–September period of 2021, when the study was conducted. Variations in temperature and relative humidity during the vegetation period are presented in Figure 2.

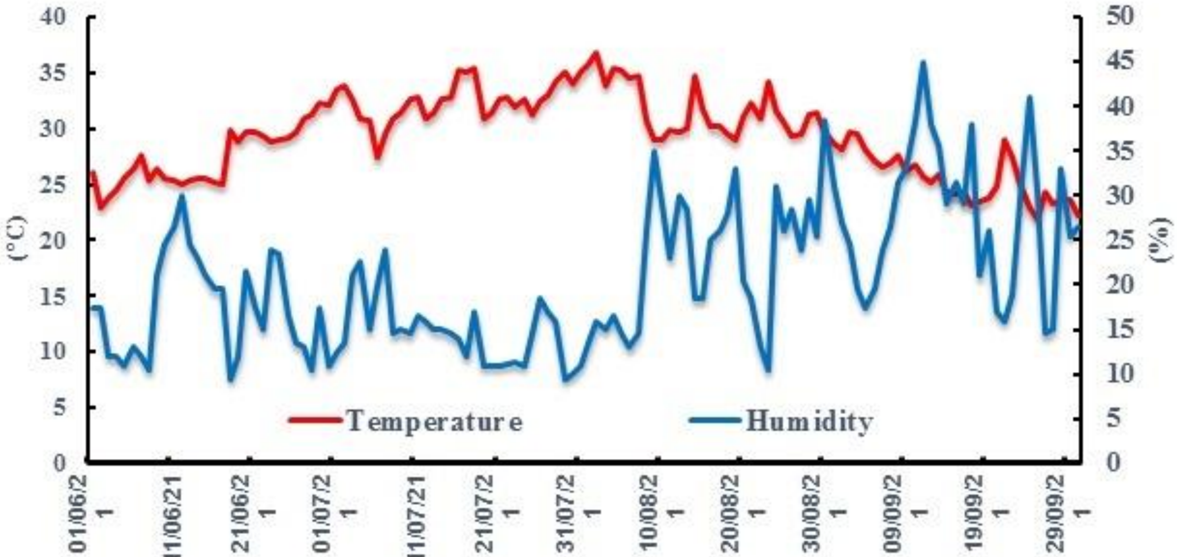

Figure 2. Vegetation Period (June-September) Temperature and Humidity Values

NDVI Measurement: NDVI measurements were carried out using the GreenSeeker (GS), an active optical sensor. Because the GS uses its own light source, it reduces the effect of ambient light variability and allows measurements to be taken under both daytime and nighttime conditions. The device employs two optical sensors operating in the visible region (660 ± 20 nm) and the near-infrared region (780 ± 25 nm). Measurement dates were determined according to the phenological development stages of cotton and were scheduled to represent emergence, the onset of squaring, the onset of flowering, the onset of boll opening, and maturity. Measurements were taken between 10:00 and 14:00 in accordance with the manufacturer's instructions, with the GS held approximately 0.7–1.0 m above the target surface. In each plot, four readings were collected from different points, including two along the row direction and two perpendicular to the row direction, and the mean of these readings was used as the NDVI value for the respective plot (Pradhan *et al.,* 2018).

Satellite Image Processing and Derivation of Vegetation Indexes: Spectral data for the study area were obtained from Sentinel-2 Level-2A surface reflectance (SR) imagery available in the Google Earth Engine environment (COPERNICUS/S2_SR_HARMONIZED). These data contain surface reflectance values atmospherically corrected using the Sen2Cor algorithm. During preprocessing, cloud, shadow, and cirrus effects were masked using the QA60 and SCL bands, and a scaling factor of 1/10,000 was then applied to convert spectral values to the 0–1 range. Bands with different spatial resolutions (10, 20, and 60 m) were resampled using the nearest-neighbor method in order to align them to a common grid structure. The image archive was spatially filtered according to the coordinates of the study area, and multispectral images corresponding to cotton phenology were selected. Field observations were acquired on the same dates as satellite overpasses, except for the field observation on 5 July 2021, for which the satellite image from the following day was used. To ensure data quality, an image-level cloud cover threshold of 10% was applied. Plot boundaries were delineated based on cadastral data, and a 20 m inward buffer was applied to reduce edge effects and spectral mixing from neighboring pixels. For each sampling date, mean band reflectance values of valid pixels within the buffered area were calculated using zonal statistics, and the final analytical dataset was generated from these values. Because of cloud contamination in the image acquired on 12 August 2021, spectral data could not be obtained for five plots, and these observations were excluded from the relevant analyses. The spectral and spatial characteristics of the Sentinel-2 bands used in the study are presented in Table 2. The extracted band values were organized in Microsoft Excel, and the vegetation indices (VIs) used in this study were calculated according to the formulas given in Table 3. The calculated index values were subsequently analyzed in JMP 5.0.1 (SAS Institute Inc., Cary, NC, USA) to evaluate their relationships with field-measured NDVI.

Table 2. Technical characteristics of the Sentinel-2 bands, including band designation, central wavelength, and spatial resolution.

Band Name	Central Wavelength (nm)	Spatial resolution (m)
B1 – Coastal Aerosol	443	60
B2 – Blue	490	10
B3 – Green	590	10
B4 – Red	665	10
B5 – Red Edge	705	20
B6 – Red Edge	740	20
B7 – Red Edge	783	20
B8 – NIR	842	10
B8A – Red Edge	865	20
B9 – Water Vapor	945	60
B10 – Cirrus	1375	60
B11 – SWIR	1610	20
B12 – SWIR	2190	20

B= band; NIR= Near-İnfrared; SWIR= Short-Wave İnfrared; nm= Nanometer; m= Meter.

Table 3. Spectral indices used in this study, including their formulas, main characteristics, and literature sources.

Index	Formula	Characteristic	Reference
ARVI	(B8 − B4 − 1 × (B4 − B2)) / (B8 + B4 − 1 × (B4 − B2))	Resistant to atmospheric effects	(Kaufman and Tanre, 1992)
GARI	(B8 - (B3 - (B2- B4))) / (B8 - (B3 + (B2- B4)))	Resistant to atmospheric effects	(Gitelson *et al.*1996)
EVI 2	2.4 × ((B8 − B4) / (B8 + B4 + 1))	Sensitive to canopy structure / vegetation density	(Jiang *et al.,* 2008)
MTVI2	(1.5 × ((1.2 × (B8 − B3) − 2.5 × (B4 − B3)) / (√ (((2 × B8 + 1) ^2) − (6 × B8 − 5 × √B4) − 0.5)))	Sensitive to canopy structure / vegetation density	(Haboudane, 2004)
MNDVI	(B8A – B11) / (B8A + B11)	Sensitive to plant water content / water stress	(Jurgens, 1997; Ji *et al.,* 2011)
MSI	B11/ B8	Sensitive to plant water content / water stress	(Hunt and Rock, 1989)
NDMI	(B8 – B11) / (B8 + B11)	Sensitive to plant water content / water stress	(Cibula *et al.,* 1992)
RDI	B12 / B8	Sensitive to plant water content / water stress	(Pinder and McLeod, 1999)
MRENDVI	(B6 − B5) / (B6 + B5 − 2 × B1)	Pigment / red-edge sensitive	(Datt 1999)
SIPI	(B8 - B2) / (B8 - B4)	Pigment / red-edge sensitive	(Penuelas *et al.,* 1995)
SAVI	((B8 − B4) / (B8 + B4 + L)) × (1 + L)	Resistant to soil background effect	(Huete, 1988)
MSAVI	((2 × B8 + 1) − (√ (((2 × B8 + 1) ^2) − (8 × (B8 − B4))))) / 2	Resistant to soil background effect	(Qi *et al.,* 1994)

B= Sentinel-2 band; L= soil adjustment factor in the SAVI formula;

The indexes used in this study were organized under functional categories according to their dominant spectral sensitivities and the biophysical properties they are intended to capture. ARVI and GARI are indexes designed to reduce atmospheric effects and thereby enable a more stable interpretation of vegetation-related reflectance signals (Kaufman and Tanre 1992; Gitelson *et al.* 1996). These characteristics make them particularly relevant for monitoring canopy development in cotton under conditions where atmospheric variability is pronounced. EVI2 and MTVI2, in contrast, are distinguished by their sensitivity to canopy structure and live vegetation density. EVI2 was developed to produce a more stable spectral response under dense vegetation conditions, whereas MTVI2 has been described as an index strongly related to green leaf area and canopy structure (Haboudane, 2004; Jiang *et al.,* 2008). This common orientation highlights their utility for tracking canopy closure, live vegetation density, and developmental differences, particularly during the early and mid-growth stages of cotton.

MNDVI, NDMI, MSI, and RDI were considered as indexes sensitive to plant water status and moisture-related variation. NIR–mid-infrared (MIR)/short-wave infrared (SWIR)-based indexes have been reported to carry information related to vegetation moisture status and to reflect changes associated with leaf water content and moisture stress (Hunt and Rock, 1989; Gao, 1996; Ji *et al.,* 2011). This shared spectral sensitivity makes these indexes particularly useful for monitoring water status, moisture balance, and drought-related patterns in cotton, especially in the context of irrigation planning, early detection of water stress, and evaluation of within-field moisture variability (Kaplan *et al.,* 2023; Sapkota *et al.,* 2024; Ben-Gal *et al.,* 2025). SIPI and MRENDVI were interpreted under the category of pigment/red-edge-sensitive indexes because of their potential to reflect variation related to pigment composition and chlorophyll status. SIPI is particularly sensitive to the carotenoid/chlorophyll-a ratio, whereas MRENDVI is more responsive to chlorophyll and leaf condition through changes in the red-edge region (Penuelas *et al.,* 1995; Datt, 1998). These properties support considering the two indexes together in the assessment of pigment status, chlorophyll dynamics, and physiological variation in cotton. SAVI and MSAVI were likewise treated as indexes aimed at reducing soil background effects (Huete, 1988; Qi *et al.,* 1994). Their greater usefulness during early growth stages, when vegetation cover is sparse and soil contribution to reflectance is more pronounced, makes them particularly suitable for evaluating early growth patterns and within-field heterogeneity in cotton. This functional classification was adopted to interpret the indexes not as equivalent measures repeating the same information, but as shared or complementary sources of information representing different biophysical properties in cotton.

Plot Characteristics and Management Practices: Field observations were conducted five times during the growing season, taking crop growth, phenological stages, and satellite overpass dates into account. Cotton was planted in the plots at a spacing of 10 × 70 cm (within-row × between-row). In addition, irrigation was applied 8–10 times, pesticide application and hoeing were performed 3–4 times, and fertilization was carried out twice. The study was conducted under farmer-managed conditions, and no additional or special treatments were imposed. Information on the monitored plots is presented in Table 4.

Table 4. Field-level agronomic and management characteristics of the sampled cotton fields, including cultivar, sowing-harvest dates, growing period, irrigation method, and within-row/row spacing.

Field ID	Cultivar	Sowing-Harvest Dates	Growing period (days)	Irrigation method	Within-Row / Row Spacing (cm)
P01	MAY 455	03.05-29.09.2021	149	Sprinkler irrigation	10 × 70
P02	MAY 455	03.05-29.09.2021	149	Sprinkler irrigation	10 × 70
P03	MAY 455	05.05-01.10.2021	149	Sprinkler irrigation	10 × 70
P04	MAY 455	06.05-02.10.2021	149	Sprinkler irrigation	10 × 70
P05	MAY 455	03.05-03.10.2021	153	Drip irrigation	10 × 70
P06	MAY 455	04.05-04.10.2021	153	Sprinkler irrigation	10 × 70
P07	MAY 455	05.05-05.10.2021	153	Sprinkler irrigation	10 × 70
P08	MAY 455	15.04-19.09.2021	157	Sprinkler irrigation	10 × 70
P09	MAY 455	21.04-20.09.2021	152	Sprinkler irrigation	10 × 70
P10	MAY 455	05.05-20.10.2021	168	Drip irrigation	10 × 70
P11	MAY 455	05.05-20.10.2021	168	Drip irrigation	10 × 70
P12	FIONA	23.04-29.09.2021	159	Drip irrigation	10 × 70
P13	FIONA	24.04-30.09.2021	159	Drip irrigation	10 × 70
P14	FIONA	25.04-29.09.2021	157	Drip irrigation	10 × 70
P15	FIONA	20.04-01.10.2021	164	Drip irrigation	10 × 70
P16	FIONA	26.04-02.10.2021	159	Drip irrigation	10 × 70
P17	MAY 455	23.04-14.10.2021	174	Drip irrigation	10 × 70
P18	MAY 455	24.04-15.10.2021	174	Drip irrigation	10 × 70
P19	FIONA	25.04-03.10.2021	161	Drip irrigation	10 × 70

P20	MAY 455	27.04-07.10.2021	163	Drip irrigation	10 × 70
P21	MAY 455	20.04-12.10.2021	175	Drip irrigation	10 × 70
P22	CANDIA	23.04-13.10.2021	173	Drip irrigation	10 × 70
P23	MAY 455	21.04-03.10.2021	165	Drip irrigation	10 × 70
P24	MAY 455	22.04-04.10.2021	165	Drip irrigation	10 × 70
P25	MAY 455	23.04-10.10.2021	170	Drip irrigation	10 × 70
P26	LIMA	22.04-16.10.2021	177	Drip irrigation	10 × 70
P27	FIONA	23.04-15.10.2021	175	Drip irrigation	10 × 70

Field ID indicates the sampled field code. Sowing-harvest dates are presented as day.month.year–day.month.year. Growing period is expressed in days. Within-row/row spacing is given as within-row spacing × row spacing (cm).

Classification of Phenological Periods: Cotton passes through distinct phenological stages during the growing season, and these stages may lead to substantial changes in the structural and spectral properties of the canopy (Oosterhuis and Jernstedt, 1999). The stage characterized mainly by vegetative growth and rapid canopy expansion was defined as the early season, and observations collected on 18 June and 5 July 2021 were assigned to this period. The stage marked by the onset of flowering, accelerated boll formation, and maximum canopy development was classified as the mid-season, including observations from 28 July and 12 August 2021. The stage in which boll development was largely completed, boll opening had begun, and the crop had entered the maturation phase was defined as the late season, represented by the observation collected on 6 September 2021. This phenological classification was used in the stage-based regression models to evaluate how the relationships between VIs and NDVI changed over the growing season. The NDVI distributions for the five observation dates representing cotton phenology are presented in Figure 3.

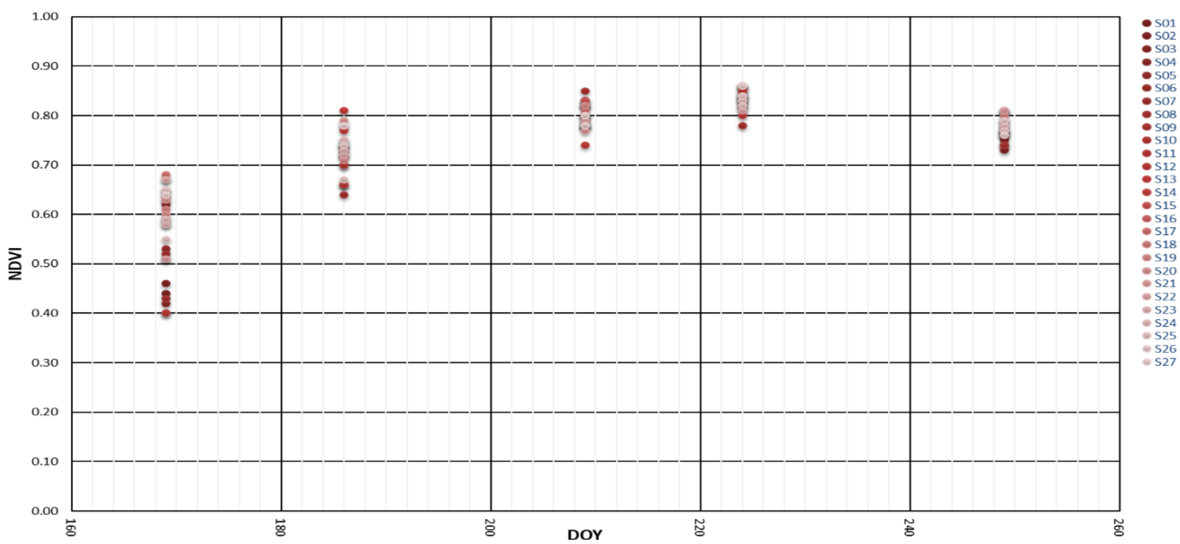

Figure 3. Distribution of GreenSeeker-derived NDVI values across five sampling dates grouped by phenological stage.

Statistical Analysis: The linear relationship between each vegetation index and field-measured NDVI was evaluated using regression analysis, both for the full dataset and separately for each phenological stage. To examine whether the index–NDVI relationship changed across phenological stages, models were fitted for each index including the main effects of index and stage, as well as the index × stage interaction. Bland–Altman analysis was used to assess agreement at the observation level and to quantify systematic differences, and bias together with the 95% limits of agreement (bias ± 1.96 SD) were reported. Because the indices differed in scale and variance structure, the variables were standardized before the Bland–Altman and PCA analyses to ensure comparability. The shared and divergent variation structure among indices was evaluated using principal component analysis (PCA) based on the standardized correlation matrix.

RESULTS

Field-measured NDVI and satellite-derived vegetation indices were compared using regression analysis, Bland–Altman agreement analysis, and principal component analysis (PCA). Stage-specific regressions were performed for the early, mid, and late phenological periods, and season-long regressions were calculated using pooled observations across the full growing season. In addition, regression models including phenological stage and stage × index interaction terms were fitted for the main functional index groups. Bland–Altman analysis was used to quantify mean differences (bias) and 95% limits of agreement between NDVI and each index. PCA was applied to summarize the multivariate structure of NDVI and the tested indices.

NDVI values were low at the beginning of the season, increased during crop development, and declined during boll opening and maturity (Figure 3). The relationships between field-measured NDVI and the tested vegetation indices were evaluated using regression, Bland–Altman, and PCA analyses (Tables 5–13; Figures 4–9).

Stage-specific regressions showed that the relationships between NDVI and the indices varied across the growing season (Table 5). For all indices, the highest R^2 values were observed during the early period ($R^2 = 0.71–0.76$), whereas lower R^2 values were obtained during the mid period ($R^2 = 0.03–0.20$) and late period ($R^2 = 0.01–0.04$). Season-long regressions produced higher R^2 values overall ($R^2 = 0.76–0.84$).

Table 5. R^2 values for the relationships between NDVI and the spectral indices during early, mid, late, and season-long periods.

Index	Early R^2	Mid R^2	Late R^2	Season-long R^2
ARVI	0.74**	0.18**	0.04**	0.83**
EVI2	0.71**	0.19**	0.03**	0.81**
GARI	0.76**	0.04**	0.04**	0.84**
MNDVI	0.74**	0.20**	0.03**	0.80**
MRENDVI	0.76**	0.03**	0.01**	0.80**
MSAVI	0.73**	0.18**	0.03**	0.83**
MSI	0.74**	0.14**	0.02**	0.81**
MTVI2	0.74**	0.17**	0.02**	0.84**
NDMI	0.72**	0.14**	0.02**	0.76**
RDI	0.75**	0.19**	0.03**	0.83**
SAVI	0.71**	0.19**	0.03**	0.81**
SIPI	0.71**	0.05**	0.03**	0.80**

R^2= coefficient of determination; **= indicates statistical significance at $P < 0.01$. Early, mid, and late denote the defined growth-stage periods used in the analysis. Season-long refers to the analysis performed using observations pooled across the full study period.

Bland–Altman analysis showed differences in agreement between NDVI and the tested indices (Table 6). MTVI2 (bias = 0.00; limits of agreement: -0.18 to 0.18) and MSAVI (bias = -0.07; limits of agreement: -0.19 to 0.04) showed the smallest mean differences and the narrowest agreement intervals. ARVI (bias = 0.07; limits of agreement: -0.18 to 0.32) and GARI (bias = -0.10; limits of agreement: -0.30 to 0.10) also showed relatively narrow agreement intervals. Wider agreement intervals were observed for NDMI, RDI, MSI, SIPI, and EVI2 (Table 6).

Table 6. Bias and limits of agreement from the Bland–Altman analysis comparing NDVI with the Vis

	ARVI	**EVI2**	**GARI**	**MNDVI**	**MRENDVI**	**MSAVI**	**MSI**	**MTVI2**	**NDMI**	**RDI**	**SAVI**	**SIPI**
Bias	0.07	-0.94	-0.10	0.20	0.22	-0.07	0.20	0.00	0.42	0.41	-0.31	-0.38
Standard Deviation	0.13	0.32	0.10	0.11	0.07	0.06	0.28	0.09	0.07	0.29	0.17	0.28
Upper Limit	0.32	-0.30	0.10	0.40	0.35	0.04	0.75	0.18	0.56	0.97	0.03	0.16
Lower Limit	-0.18	-1.57	-0.30	-0.01	0.09	-0.19	-0.35	-0.18	0.28	-0.15	-0.64	-0.93

Bias was calculated as the mean difference between NDVI and each spectral index. Standard deviation refers to the standard deviation of the pairwise differences. Upper and lower limits represent the 95% limits of agreement. Vis: vegetation index.

PCA indicated that the first principal component explained 96.73% of the total variance, whereas PC2 explained 1.60% and the remaining components contributed marginally (Table 7). Loading values showed similar positive contributions on PC1 for ARVI, EVI2, GARI, MNDVI, MRENDVI, MSAVI, MTVI2, NDMI, and SAVI, whereas MSI, RDI, and SIPI showed negative loadings on PC1. The loading plot showed that NDVI was oriented similarly to ARVI, MSAVI, MTVI2, MNDVI, and MRENDVI, while MSI, RDI, and SIPI were positioned in the opposite direction (Table 8; Figure 4).

Table 7. Eigenvalues, explained variance, and cumulative explained variance of the principal components obtained from the Vis

Principal Component	Eigenvalue	Variance (%)	Cumulative Variance (%)
PC1	12.5753	96.73	96.73
PC2	0.2077	1.6	98.33
PC3	0.1198	0.92	99.25
PC4	0.0585	0.45	99.7
PC5	0.0228	0.18	99.88

Only the first five principal components are reported, as they collectively explain 99.88% of the total variance; the contribution of the remaining components was negligible.

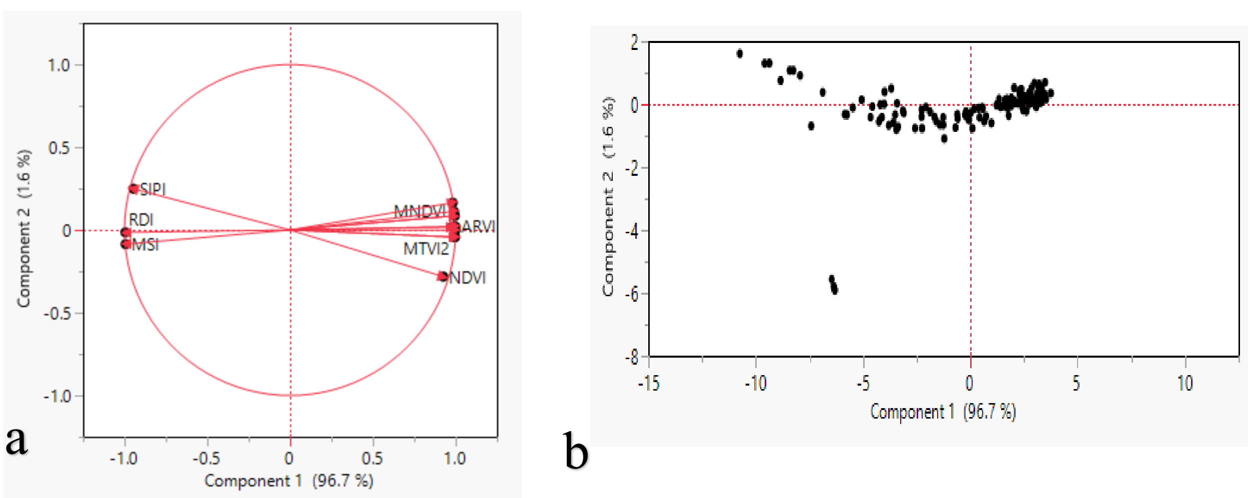

Figure 4. Principal component analysis (PCA) results for the VIs. (a) The loading plot illustrates the multivariate relationship structure among the indexes. (b) The score plot illustrates the distribution of observations across the PCA axes.

Table 8. Principal component loadings for NDVI and the VIs across the first 12 principal components.

	PC1	PC2	PC3	PC4	PC5	PC6	PC7	PC8	PC9	PC10	PC11	PC12
NDVI	0.26	-0.62	0.74	-0.04	0.02	-0.06	0.02	-0.01	-0.01	0.01	-0.01	0.00
ARVI	0.28	0.05	-0.05	0.07	0.27	0.02	0.05	0.01	-0.11	-0.20	0.58	0.66
EVI2	0.28	0.19	0.06	0.12	0.40	-0.03	0.01	0.18	-0.06	-0.28	-0.24	-0.19
GARI	0.28	-0.09	-0.16	-0.06	-0.19	0.45	0.79	0.07	-0.05	0.02	-0.10	-0.02
MNDVI	0.28	0.25	0.14	-0.25	-0.18	0.20	-0.19	0.48	0.41	0.13	0.42	-0.28
MRENDVI	0.28	0.04	-0.01	0.83	-0.47	-0.02	-0.13	0.01	0.00	0.01	0.01	-0.01
MSAVI	0.28	0.00	-0.12	0.04	0.30	0.06	-0.12	-0.04	-0.40	0.78	0.05	-0.13

MSI	-0.28	-0.19	-0.02	0.24	0.25	0.26	-0.05	0.50	0.35	0.25	-0.31	0.40
MTVI2	0.28	-0.09	-0.18	0.04	0.24	0.11	-0.07	-0.60	0.66	0.07	-0.05	-0.04
NDMI	0.28	0.36	0.15	-0.20	-0.20	-0.55	0.19	0.04	0.17	0.25	-0.34	0.37
RDI	-0.28	-0.03	0.03	0.30	0.26	-0.46	0.50	0.09	0.22	0.14	0.38	-0.29
SAVI	0.28	0.19	0.06	0.12	0.40	-0.03	0.01	0.18	-0.06	-0.28	-0.24	-0.19
SIPI	-0.27	0.55	0.58	0.15	0.09	0.39	0.12	-0.30	-0.02	0.11	0.03	0.06

Loading values indicate the contribution and direction of each index to each principal component. NDVI was included together with the spectral indices in the PCA.

PCA and Bland–Altman analyses summarized the overall multivariate pattern and agreement structure among NDVI and the tested indices. To evaluate whether these relationships varied by phenological stage, additional regression analyses including stage effects were performed. The indices were analyzed in functional groups.

Within the group of atmospherically resistant indices, both ARVI and GARI showed high model fit (ARVI: $R^2 = 0.859$; GARI: $R^2 = 0.867$), and both models were significant overall ($p < 0.0001$). The main effect of the index was significant in both models, whereas the main effect of phenological stage was significant only for GARI ($p = 0.0472$). The stage × index interaction was significant for both indices (ARVI: $p = 0.0001$; GARI: $p = 0.0050$). In the ARVI model, both the EARLY × index and LATE × index interaction terms were significant, whereas in the GARI model only the EARLY × index term was significant (Table 9).

Table 9. Regression analysis results for the relationships between atmospherically resistant indexes (ARVI and GARI) and NDVI, including the effect of phenological stage

Index	**ARVI**	**GARI**
R²	0.859	0.867
Adj. R²	0.854	0.862
RMSE	0.041	0.04
F	151.59	161.81
Model p	<0.0001	<0.0001
Index p	<0.0001	0.0017
STAGE p	0.2201	0.0472
STAGE× Index p	0.0001	0.005
Early β (p)	-0.0155 (0.116)	-0.0239 (0.046)
Late β (p)	-0.0014 (0.912)	-0.0064 (0.722)
Early× Index β (p)	0.2512 (<0.0001)	0.2731 (0.002)
Late× Index β (p)	-0.1879 (0.047)	-0.1539 (0.278)

MID was used as the reference phenological stage; the EARLY and LATE coefficients indicate differences relative to MID. R^2 = proportion of variance explained by the model; β = regression coefficient; F = overall model significance test; p = probability value.

Figures 5a and 5b show the overall and stage-specific relationships of ARVI and GARI with NDVI. Figure 5a indicates that both indices had positive linear relationships with NDVI when all observations were analyzed together, with high overall explanatory power for both models. Figure 5b shows that these relationships differed across phenological stages. For both indices, the relationship was stronger in the early period and weaker in the mid and late periods. For ARVI, R^2 decreased from 0.74 in the early period to 0.18 and 0.03 in the mid and late periods, respectively. Similarly, for GARI, R^2 was 0.76 in the early period, whereas the explanatory power remained limited in the mid and late periods. This pattern was consistent with the significant stage × index interactions reported in Table 9.

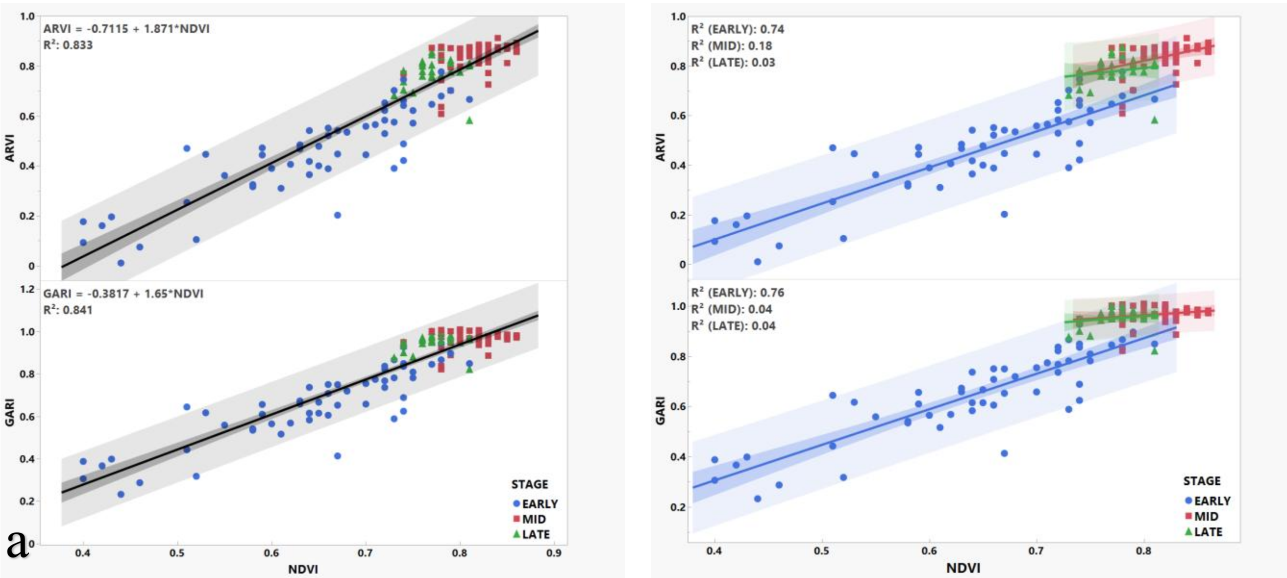

Figure 5. Phenological variation in the relationships between atmospherically resistant VIs (ARVI and GARI) and NDVI. (a) Overall linear relationships between NDVI and ARVI/GARI. Points are colored according to phenological stage, and the black line represents the fitted regression line for all observations. (b) Stage-specific regression relationships between NDVI and ARVI/GARI. Lines represent the linear fit for each phenological stage, and the shaded areas indicate the confidence intervals.

Within the group of indices sensitive to canopy structure and live vegetation density, both EVI2 and MTVI2 showed high model fit (R^2 = 0.851–0.860), and both models were significant overall ($p < 0.0001$) (Table 10). The main effect of the index was significant in both models, whereas the main effect of phenological stage was significant only for MTVI2 ($p = 0.0336$). The stage × index interaction was significant for both indices (EVI2: $p < 0.0001$; MTVI2: $p = 0.0040$). The EARLY × index interaction term was significant in both models, whereas the LATE × index interaction term was significant only for EVI2 (Table 10).

Table 10. Regression analysis results for the relationships between canopy structure and live vegetation density-sensitive indexes (EVI2 and MTVI2) and NDVI, including the effect of phenological stage

Index	EVI2	MTVI2
R^2	0.851	0.86
Adj. R^2	0.845	0.854
RMSE	0.042	0.041
F	141.19	152.08
Model p	<0.0001	<0.0001
Index p	<0.0001	0.0002
STAGE p	0.48	0.0336
STAGE× Index p	<0.0001	0.004
Early β (p)	-0.0082 (0.400)	-0.0256 (0.012)
Late β (p)	-0.0059 (0.620)	0.0050 (0.715)
Early× Index β (p)	0.1537 (<0.0001)	0.2625 (0.001)
Late× Index β (p)	-0.1052 (0.019)	-0.2247 (0.085)

MID was used as the reference phenological stage; the EARLY and LATE coefficients indicate differences relative to MID. R^2 = proportion of variance explained by the model; β = regression coefficient; F = overall model significance test; p = probability value.

Figures 6a and 6b show the overall and stage-specific relationships of EVI2 and MTVI2 with NDVI. Figure 6a indicates that both indices had positive linear relationships with NDVI when all observations were considered together. Figure 6b shows that these relationships varied across phenological stages. For both indices, the relationship was stronger in the early period and weaker in the mid and late periods. The early-period R^2 values were 0.71 for EVI2 and

0.74 for MTVI2, whereas lower R^2 values were obtained in the mid and late periods. This pattern was consistent with the significant stage × index interactions reported in Table 10.

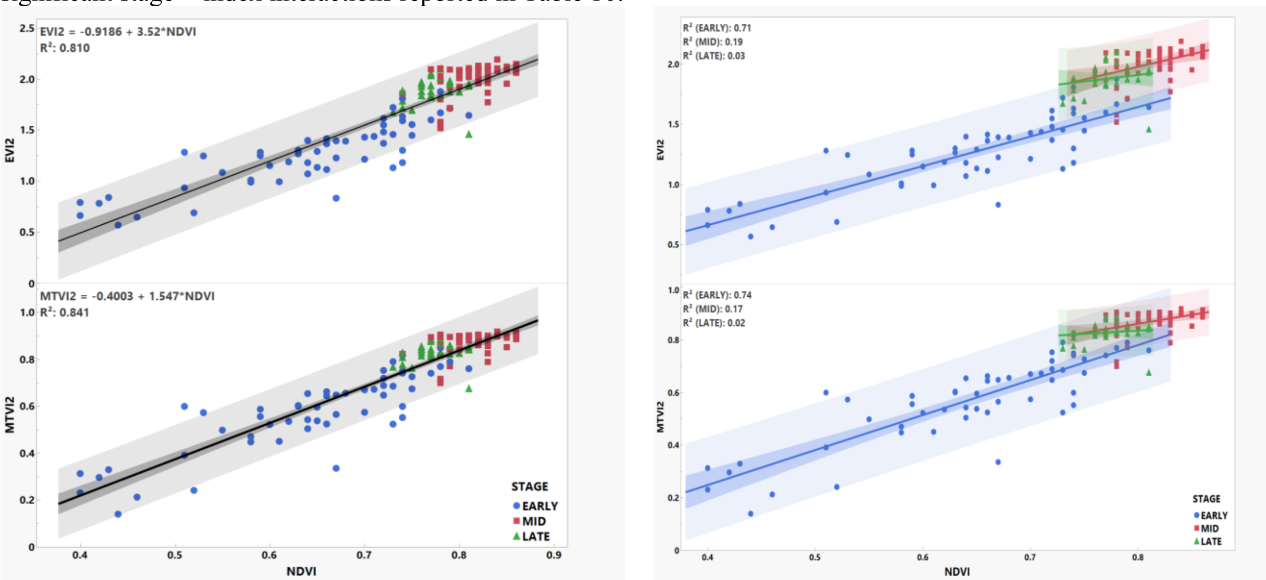

Figure 6. Phenological variation in the relationships between canopy structure and vegetation density-sensitive indexes (EVI2 and MTVI2) and NDVI. (a) Overall linear relationships between NDVI and EVI2/MTVI2. Points are colored according to phenological stage, and the black line represents the fitted regression line for all observations. (b) Stage-specific regression relationships between NDVI and EVI2/MTVI2. Lines represent the linear fit for each phenological stage, and the shaded areas indicate the confidence intervals.

Within the group of water content- and moisture-sensitive indices, MNDVI, NDMI, MSI, and RDI all showed high model fit (R^2 = 0.852–0.866), and all models were significant overall ($p < 0.0001$) (Table 11). The main effect of the index was significant in all four models, whereas the main effect of phenological stage was not significant in any model. The stage × index interaction was significant for all four indices. For MNDVI and NDMI, the EARLY × index interaction terms were positive and significant, whereas the LATE × index interaction terms were negative and significant. In contrast, MSI and RDI showed negative and significant EARLY × index interaction terms and positive and significant LATE × index interaction terms (Table 11).

Table 11. Regression analysis results for the relationships between water content- and moisture-sensitive indexes (MNDVI, MSI, RDI, and NDMI) and NDVI, including the effect of phenological stage

Index	MNDVI	NDMI	MSI	RDI
R²	0.86	0.852	0.859	0.866
Adj. R²	0.854	0.846	0.853	0.861
RMSE	0.041	0.042	0.041	0.04
F	152.44	142.81	150.87	160.24
Model p	<0.0001	<0.0001	<0.0001	<0.0001
Index p	<0.0001	<0.0001	<0.0001	<0.0001
STAGE p	0.702	0.445	0.52	0.34
STAGE× Index p	<0.0001	<0.0001	<0.0001	0.0017
Early β (p)	-0.0005 (0.957)	0.0063 (0.534)	-0.0080 (0.432)	-0.0143 (0.186)
Late β (p)	-0.0096 (0.469)	-0.0152 (0.205)	-0.0061 (0.640)	-0.0000 (0.998)
Early× Index β (p)	0.3514 (<0.0001)	0.5638 (<0.0001)	-0.3584 (<0.0001)	-0.2679 (0.0004)
Late× Index β (p)	-0.2537 (0.006)	-0.3669 (0.0005)	0.2635 (0.0062)	0.2396 (0.0425)

MID was used as the reference phenological stage; the EARLY and LATE coefficients indicate differences relative to MID. R^2 = proportion of variance explained by the model; β = regression coefficient; F = overall model significance test; p = probability value.

Figure 7a shows positive linear relationships of MNDVI and NDMI with NDVI and negative linear relationships of MSI and RDI with NDVI. Figure 7b shows that these relationships varied across phenological stages. For all four indices, within-stage explanatory power was higher in the early period and lower in the mid and late periods. This pattern was consistent with the significant stage × index interactions reported in Table 11.

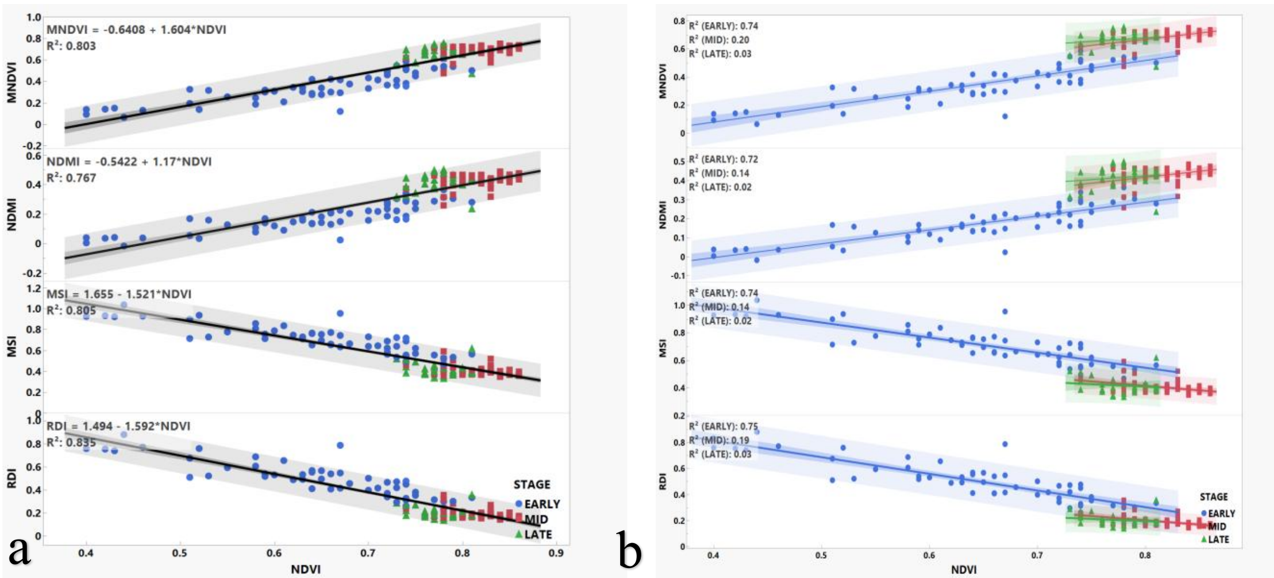

Figure 7. Phenological variation in the relationships between water content- and moisture-sensitive indexes (MNDVI, NDMI, MSI, and RDI) and NDVI. (a) Overall linear relationships between NDVI and MNDVI, NDMI, MSI, and RDI. Points are colored according to phenological stage, and the black line represents the fitted regression line for all observations. (b) Stage-specific regression relationships between NDVI and MNDVI, NDMI, MSI, and RDI. Lines represent the linear fit for each phenological stage, and the shaded areas indicate the confidence intervals.

Within the group of pigment/red-edge-sensitive indices, both SIPI and MRENDVI showed high model fit (SIPI: R^2 = 0.848; MRENDVI: R^2 = 0.865), and both models were significant overall ($p < 0.0001$) (Table 12). The main effect of the index was significant for MRENDVI ($p < 0.0001$) but not for SIPI ($p = 0.0625$). The main effect of phenological stage was significant in both models (SIPI: $p = 0.0268$; MRENDVI: $p = 0.0006$). The stage × index interaction was significant only for MRENDVI ($p < 0.0001$) and not for SIPI ($p = 0.7008$) (Table 12).

Table 12. Regression analysis results for the relationships between pigment/red-edge-sensitive indexes (SIPI and MRENDVI) and NDVI, including the effect of phenological stage

Index	**SIPI**	**MRENDVI**
R²	0.848	0.865
Adj. R²	0.842	0.86
RMSE	0.042	0.04
F	138.89	159.23
Model p	<0.0001	<0.0001
Index p	0.0625	<0.0001
STAGE p	0.0268	0.0006
STAGE× Index p	0.7008	<0.0001
Early β (p)	-0.0424 (0.0138)	-0.0315 (0.0001)
Late β (p)	0.0065 (0.8140)	-0.0009 (0.9112)
Early× Index β (p)	-0.1383 (0.4000)	0.4690 (<0.0001)
Late× Index β (p)	0.1287 (0.6444)	-0.2674 (0.0039)

MID was used as the reference phenological stage; the EARLY and LATE coefficients indicate differences relative to MID. R^2 = proportion of variance explained by the model; β = regression coefficient; F = overall model significance test; p = probability value.

Figure 8a shows the overall relationships of SIPI and MRENDVI with NDVI. SIPI showed a negative linear relationship with NDVI, whereas MRENDVI showed a positive linear relationship. Figure 8b shows these relationships across phenological stages. For both indices, within-stage explanatory power was higher in the early period (SIPI: R^2 = 0.72; MRENDVI: R^2 = 0.76) and lower in the mid and late periods. For MRENDVI, the stage-specific pattern was consistent with the significant stage × index interaction reported in Table 12.

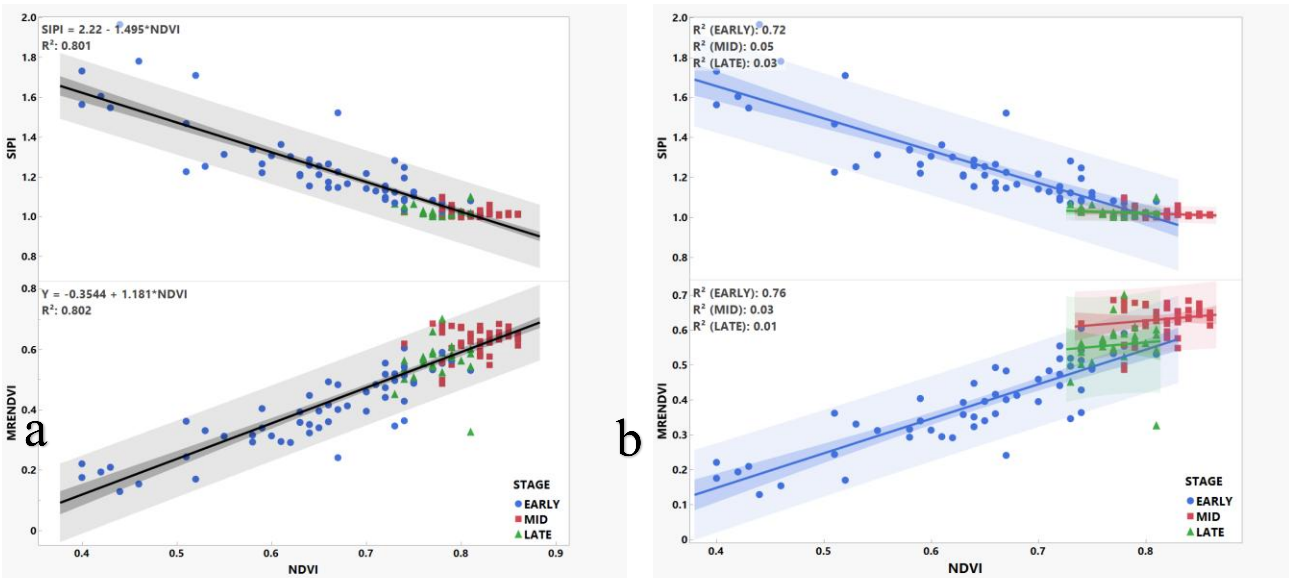

Figure 8. Phenological variation in the relationships between pigment-sensitive indexes (SIPI and MRENDVI) and NDVI. (a) Overall linear relationships between NDVI and SIPI/MRENDVI. The black line represents the fitted regression line for all observations. (b) Stage-specific regression relationships between NDVI and SIPI/MRENDVI. Points represent phenological stages, and the shaded areas indicate the confidence intervals.

Within the group of soil background-resistant indices, both SAVI and MSAVI showed high model fit (SAVI: R^2 = 0.851; MSAVI: R^2 = 0.855), and both models were significant overall ($p < 0.0001$) (Table 13). In both models, the main effect of the index was significant ($p < 0.0001$), whereas the main effect of phenological stage was not significant (SAVI: p = 0.48; MSAVI: p = 0.128). The stage × index interaction was significant for both SAVI ($p < 0.0001$) and MSAVI (p = 0.001) (Table 13).

Table 13. Regression analysis results for the relationships between soil background-resistant indexes (SAVI and MSAVI) and NDVI, including the effect of phenological stage

Index	**SAVI**	**MSAVI**
R^2	0.851	0.855
Adj. R^2	0.845	0.849
RMSE	0.042	0.042
F	141.19	145.92
Model p	<0.0001	<0.0001
Index p	<0.0001	<0.0001
STAGE p	0.48	0.128
STAGE× Index p	<0.0001	0.001
Early β (p)	-0.0082 (0.3997)	-0.0196 (0.0533)
Late β (p)	-0.0059 (0.6201)	0.0016 (0.9028)
Early× Index β (p)	0.2459 (<0.0001)	0.3724 (0.0002)
Late× Index β (p)	-0.1683 (0.0185)	-0.3003 (0.0614)

MID was used as the reference phenological stage; the EARLY and LATE coefficients indicate differences relative to MID. R^2 = proportion of variance explained by the model; β = regression coefficient; F = overall model significance test; p = probability value.

Figure 9a shows the overall linear relationships of SAVI and MSAVI with NDVI. Both indices showed strong positive linear relationships with NDVI. Figure 9b shows that these relationships varied across phenological stages. For both indices, within-stage explanatory power was higher in the early period (SAVI: $R^2 = 0.71$; MSAVI: $R^2 = 0.72$) and lower in the mid and late periods. Regression slopes also differed among stages. This pattern was consistent with the significant stage × index interactions reported in Table 13.

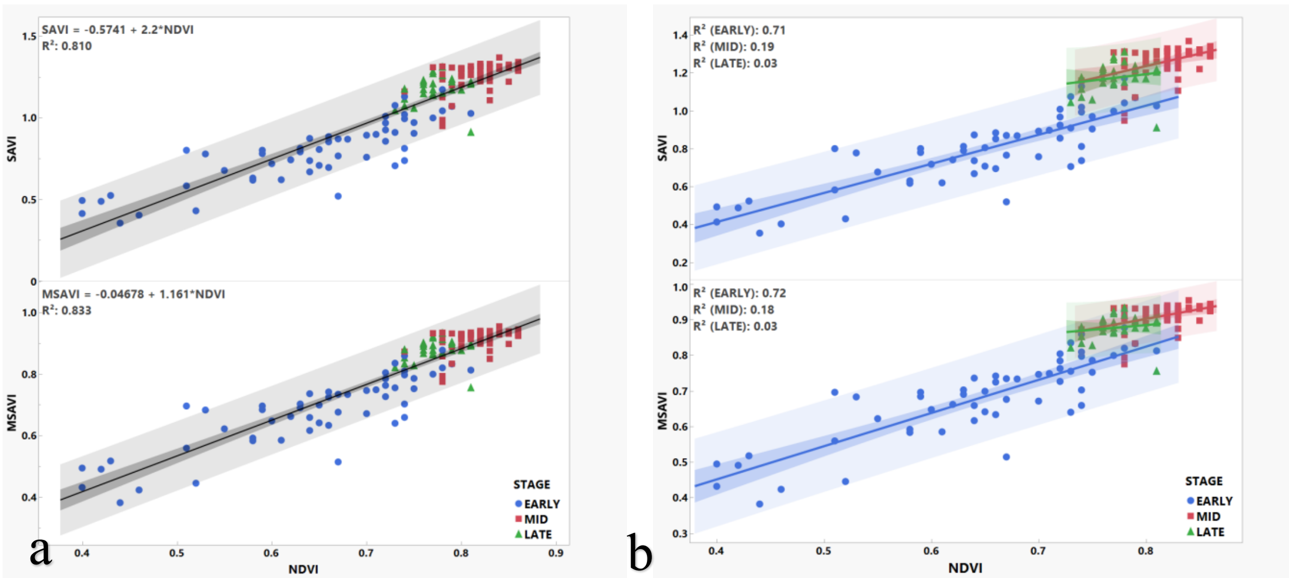

Figure 9. Phenological variation in the relationships between soil background-resistant indexes (SAVI and MSAVI) and NDVI. (a) Overall linear relationships between NDVI and SAVI/MSAVI. The black line represents the fitted regression line for all observations. (b) Stage-specific regression relationships between NDVI and SAVI/MSAVI. Points represent phenological stages, and the shaded areas indicate the confidence intervals.

Overall, the combined regression, Bland–Altman, and PCA results indicated that the relationships between NDVI and the evaluated vegetation indices were not uniform across index groups or phenological stages. Although many regression models showed relatively high explanatory power ($R^2 \approx 0.80$–0.87), significant stage × index interactions in multiple models pointed to stage-dependent variation in these relationships. Bland–Altman analysis identified lower bias and narrower limits of agreement for MTVI2, MSAVI, ARVI, and GARI, whereas NDMI, RDI, MSI, SIPI, and EVI2 showed comparatively wider agreement intervals. PCA results likewise showed that several indices were aligned within a common multivariate pattern, whereas others were separated from NDVI in ordination space.

DISCUSSION

The present results show that relationships among vegetation indices in cotton should be interpreted within phenological context rather than as seasonally uniform patterns. Although several indices showed strong seasonal-scale relationships with field-measured NDVI, the significant stage × index interactions observed in multiple models indicate that these relationships changed across the growing season. This pattern is consistent with seasonal shifts in canopy structure, water status, and late-season canopy heterogeneity, all of which modify spectral responses over time (Ren *et al.,* 2020; Kaplan and Rozenstein, 2021; Wang *et al.,* 2023).

The strong early-season relationships and the marked decline in R^2 values during the mid and late stages indicate that NDVI and the tested indices did not track a stable spectral gradient throughout the cotton growing cycle. In the early vegetative period, canopy expansion, increasing fractional cover, and exposed soil background generate a relatively coherent structural signal, so multiple indices respond in parallel and show stronger linear relationships with NDVI. As phenological development progresses, however, this common signal weakens because spectral variation becomes partitioned among different biophysical components, including chlorophyll dynamics, canopy architecture, water status, boll development, and the increasing contribution of exposed soil and open bolls. Under these conditions, the decline in stage-specific R^2 values should not be interpreted merely as weaker statistical association, but as evidence that the indices are capturing increasingly distinct aspects of canopy condition. This stage-dependent loss of overlap also provides a rationale for a phenology-sensitive multi-index framework, particularly beyond the early vegetative stage, when a single NDVI-based relationship is no longer sufficient to represent the full range of spectral responses in cotton.

The stronger early-stage agreement of MTVI2, MSAVI, ARVI, and GARI with field-measured NDVI indicates that index performance in cotton was strongly influenced by the structural conditions of early vegetative growth. At this stage, canopy expansion is rapid, row closure is incomplete, and soil background still contributes substantially to the pixel signal. Under such conditions, the closer agreement of MSAVI and SAVI is consistent with their lower sensitivity to soil background effects, whereas the behavior of ARVI and GARI is compatible with a more stable representation of canopy-related spectral responses. The response of MTVI2 is likewise consistent with its sensitivity to canopy structure and green vegetation. Recent studies further show that phenology-sensitive multispectral monitoring can support the estimation of in-season growth parameters, nitrogen status, and canopy water status in cotton under field conditions (Lacerda *et al.,* 2022; Pei *et al.,* 2023, 2024). Taken together, the stronger early-stage agreement observed here appears particularly relevant for early-season cotton monitoring, especially for assessing stand establishment and within-field variability.

The contrast between MTVI2 and EVI2 suggests that these indices should not be treated as equivalent proxies of the same biophysical signal. MTVI2 is more closely associated with variation in green leaf area and canopy structure and may remain informative under high-LAI conditions, whereas EVI2 was designed to preserve sensitivity under dense vegetation by reducing red-band saturation and stabilizing index–LAI relationships under heterogeneous canopy conditions (Mourad *et al.,* 2020; Sun *et al.,* 2021; Endiviana *et al.,* 2022). This distinction is consistent with the present results, in which MTVI2 behaved more similarly to NDVI, while EVI2 showed a more pronounced systematic difference.

The separation of NDMI, MSI, RDI, and partly MNDVI from the NDVI axis in PCA, together with their wider limits of agreement in the Bland–Altman analysis, indicates that these indices were more sensitive to water-related variation in cotton, particularly during flowering and boll development. At these stages, spectral responses reflect not only canopy development but also plant water status and transpiration-related changes, and these periods have been associated with high water demand in cotton (Rehman *et al.,* 2021; Hou *et al.,* 2024). Recent cotton studies further show that UAV-based multispectral data can be used to estimate canopy water status and that water-sensitive indices can capture a more specific biophysical signal than NDVI (Holzman *et al.,* 2021; Pei *et al.,* 2024). Their lower overlap with NDVI should therefore be interpreted not as weaker performance, but as greater sensitivity to water-related physiological variation.

A similar distinction applies to the pigment- and red-edge-sensitive indices. MRENDVI and SIPI appear to convey information that differs from NDVI because NDVI primarily reflects general greenness and canopy cover, whereas red-edge and pigment-sensitive indices are more responsive to variation in chlorophyll content, nitrogen status, and leaf physiological condition. Recent studies have shown that leaf chlorophyll and nitrogen status in cotton can be estimated using multispectral and hyperspectral data, and that wavelengths in the red-edge region are particularly informative for this purpose (Marang *et al.,* 2021; Shanmugapriya *et al.,* 2023). Sentinel-2-based phenology studies also report that, while NDVI reflects general canopy dynamics, red-edge-based indices are more sensitive to chlorophyll-related and phenological variation (Misra *et al.,* 2020). In the present study, the significance of both the main effect and the stage × index interaction for MRENDVI indicates greater sensitivity to phenological change, whereas the absence of significant main and interaction effects for SIPI suggests a closer association with subtler variation in pigment composition than with overall vegetation density.

The late-season pattern also reflects a cotton-specific phenological feature. As boll opening begins and the proportion of green leaves declines, the canopy signal shifts away from a relatively homogeneous green-cover axis toward a mixture of leaves, bolls, and exposed soil. This helps explain why the divergence among indices became more pronounced in the late stage. Conversely, the closer agreement of SAVI and especially MSAVI with field-measured NDVI is consistent with the physical conditions of early cotton growth, when sparse vegetation cover and stronger soil background effects favour soil-adjusted indices. Under such conditions, MSAVI and related indices have been reported to produce more stable signals than conventional NDVI (Wen *et al.,* 2020; Al-Quraishi *et al.,* 2021; Kareem *et al.,* 2023).

Overall, the present findings suggest that index selection in cotton should not rely on a single performance criterion. Rather than reflecting a simple hierarchy of superiority, the tested indices appear to represent different functional dimensions that vary with phenological stage. MTVI2, MSAVI, ARVI, and GARI were more closely associated with early-stage structural development; NDMI, MSI, RDI, and MNDVI captured a stronger water-related signal; and MRENDVI and SIPI provided information more closely linked to pigment- and chlorophyll-related variation. Accordingly, a phenology-sensitive, multi-index approach appears more informative than interpretation based on a single vegetation metric. At the same time, these interpretations remain limited by the fact that the analyses were based on relationships with field-measured NDVI and were not directly validated against independent biophysical targets such as leaf water potential, chlorophyll status, nitrogen status, LAI, yield, or fiber quality. Future studies should therefore test the same framework against independent agronomic and physiological measurements in order to define the functional significance of these index groups more directly.

Conclusions: This study shows that vegetation indices in cotton should not be treated as interchangeable metrics, because their relationships with field-measured NDVI varied with phenological stage and reflected different functional dimensions of crop condition. MTVI2, MSAVI, ARVI, and GARI were more closely associated with early-stage structural development, whereas NDMI, MSI, RDI, and MNDVI captured a stronger water-related signal, and MRENDVI and SIPI reflected pigment- and chlorophyll-related variation more clearly. These findings support the use of a phenology-sensitive, multi-index framework rather than reliance on a single vegetation metric for cotton monitoring. However, because the analyses were conducted within a single year and were not directly validated against independent biophysical targets, the generalizability of the findings remains limited. Future studies should therefore test this framework across multiple years, environmental conditions, and cotton cultivars, and should integrate direct physiological and agronomic measurements to evaluate the functional significance of these index groups more explicitly.

Conflict of Interest: The authors declare no conflict of interest.

Funding and Acknowledgements: This study was supported by the Scientific Research Projects Coordination Unit of Dicle University under project number FBE.21.009. The authors gratefully acknowledge the support provided by the Scientific Research Projects Coordination Unit.

This article was derived from the doctoral dissertation entitled *"Investigation of the Potential Use of Satellite Imagery for Determining Plant–Water Relationships in Cotton (G. hirsutum L.)"* conducted by Serkan KILIÇASLAN in the Department of Field Crops, Graduate School of Natural and Applied Sciences, Dicle University.

Author Contributions

Author 1: Conceptualization, methodology, software, formal analysis, data curation, visualization, writing—original draft preparation.

Author 2: Supervision, project administration, funding acquisition, writing—review and editing.

Author 3: Validation, investigation, interpretation of results, writing—review and editing. All authors contributed to the article and approved the submitted version.

REFERENCES

Al-Quraishi, A., H. Razvanchy and H. Gaznayee (2021). A comparative study for performance of five Landsat-based vegetation indices: Their relations to some ecological and terrain variables. J. Appl. Sci. Technol. Trends 2(1): 58-67. https://doi.org/10.38094/jastt201165

Bahçeci, İ. and Ş. Aydın (2008). Mardin-Kızıltepe Ovası yarı taşınabilir yağmurlama sulama sistemlerinin bazı performans parametrelerinin belirlenmesi. Journal of the Faculty of Agriculture of Harran University (Turkiye), 12(1): 27-37. ISSN (Print): 1300-6819 ISSN (Online): 2587-1358

Ben-Gal, A., A. Barski, O. Bukris, H. Yasuor, S.A. O'Shaughnessy, N.C. Hansen, A. Peeters and Y. Cohen (2025). Dynamic approaches to precision irrigation of cotton. Precis. Agric. 26: 64. https://doi.org/10.1007/s11119-025-10261-1

Cibula, W.G., E.F. Zetka and D.L. Rickman (1992). Response of thematic mapper bands to plant water stress. Int. J. Remote Sens. 13(10): 1869-1880. https://doi.org/10.1080/01431169208904236

Datt, B. (1998). Remote sensing of chlorophyll a, chlorophyll b, chlorophyll a + b, and total carotenoid content in Eucalyptus leaves. Remote Sens. Environ. 66(2): 111-121. https://doi.org/10.1016/S0034-4257(98)00046-7

Datt, B. (1999). A new reflectance index for remote sensing of chlorophyll content in higher plants: Tests using Eucalyptus leaves. J. Plant Physiol. 154(1): 30-36. https://doi.org/10.1016/S0176-1617(99)80314-9

Defourny, P., S. Bontemps, N. Bellemans, C. Cara, G. Dedieu, E. Guzzonato and B. Koetz (2019). Near real-time agriculture monitoring at national scale at parcel resolution: Performance assessment of the Sen2-Agri automated system in various cropping systems around the world. Remote Sens. Environ. 221: 551-568. https://doi.org/10.1016/j.rse.2018.11.007

Endiviana, O.A., Y. Setiawan, H. Imantho, S.W. Sugiarto and T. Yuliawan (2022). Selecting the most optimum Sentinel-2A based vegetation index to estimate the leaf area index of three rice cultivars. J. Keteknikan Pertan. 10(3): 200-214. https://doi.org/10.19028/jtep.010.3.200-214

Gao, B.C. (1996). NDWI—A normalized difference water index for remote sensing of vegetation liquid water from space. Remote Sens. Environ. 58(3): 257-266. https://doi.org/10.1016/S0034-4257(96)00067-3

Gitelson, A.A., Y.J. Kaufman and M.N. Merzlyak (1996). Use of a green channel in remote sensing of global vegetation from EOS-MODIS. Remote Sens. Environ. 58(3): 289-298. https://doi.org/10.1016/S0034-4257(96)00072-7

Gu, H., C. Mills, G.L. Ritchie and W. Guo (2024). Water stress assessment of cotton cultivars using unmanned aerial system images. Remote Sens. 16(14): 2609. https://doi.org/10.3390/rs16142609

Güçdemir, İ.H. (2008). Tarım El Kitabı: Gübreler, Toprak Analizlerine Dayalı Gübreleme. Tarım ve Köyişleri Bakanlığı, Tarımsal Üretim ve Geliştirme Genel Müdürlüğü; Ankara, Türkiye. 1-87 pp. ISBN: 9789754072813

Haboudane, D. (2004). Hyperspectral vegetation indices and novel algorithms for predicting green LAI of crop canopies: Modeling and validation in the context of precision agriculture. Remote Sens. Environ. 90(3): 337-352. https://doi.org/10.1016/j.rse.2003.12.013

Holzman, M. E., Rivas, R. E., and Bayala, M. I. (2021). Relationship between TIR and NIR-SWIR as indicator of vegetation water availability. *Remote Sensing*, *13*(17), 3371. http://dx.doi.org/10.3390/rs13173371

Hou, X., H. Li, R. Ding and T. Du (2024). Hydraulic, morphological, and anatomical changes over the development of cotton bolls and pedicels leading to boll opening under well-watered and water deficit conditions. Environ. Exp. Bot. 228: 105996. https://doi.org/10.1016/j.envexpbot.2024.105996

Huang, S., L. Tang, J.P. Hupy, Y. Wang and G. Shao (2021). A commentary review on the use of normalized difference vegetation index (NDVI) in the era of popular remote sensing. J. For. Res. 32(1): 1-6. https://doi.org/10.1007/s11676-020-01155-1

Huete, A.R. (1988). A soil-adjusted vegetation index (SAVI). Remote Sens. Environ. 25(3): 295-309. https://doi.org/10.1016/0034-4257(88)90106-X

Hunt, E.R. and B.N. Rock (1989). Detection of changes in leaf water content using near- and middle-infrared reflectances. Remote Sens. Environ. 30(1): 43-54. https://doi.org/10.1016/0034-4257(89)90046-1

Ji, L., L. Zhang, B.K. Wylie and J. Rover (2011). On the terminology of the spectral vegetation index (NIR − SWIR)/(NIR + SWIR). Int. J. Remote Sens. 32(21): 6901-6909. https://doi.org/10.1080/01431161.2010.510811

Jiang, Z., A.R. Huete, K. Didan and T. Miura (2008). Development of a two-band enhanced vegetation index without a blue band. Remote Sens. Environ. 112(10): 3833-3845. https://doi.org/10.1016/j.rse.2008.06.006

Jurgens, C. (1997). The modified normalized difference vegetation index (mNDVI): A new index to determine frost damages in agriculture based on Landsat TM data. Int. J. Remote Sens. 18(17): 3583-3594. https://doi.org/10.1080/014311697216810

Kaplan, G., L. Fine, V. Lukyanov, N. Malachy, J. Tanny and O. Rozenstein (2023). Using Sentinel-1 and Sentinel-2 imagery for estimating cotton crop coefficient, height, and leaf area index. Agric. Water Manag. 276: 108056. https://doi.org/10.1016/j.agwat.2022.108056

Kaplan, G. and O. Rozenstein (2021). Spaceborne estimation of leaf area index in cotton, tomato, and wheat using Sentinel-2. Land 10(5): 505. https://doi.org/10.3390/land10050505

Kareem, H.H., M.H. Attaee and Z.A. Omran (2023). Evaluation the soil-adjusted vegetation indices SAVI and MSAVI for Bristol City, United Kingdom using Landsat 8-OLI through geospatial technology. Ecol. Eng. Environ. Technol. 24(7): 89-97. https://doi.org/10.12912/27197050/169749

Kaufman, Y.J. and D. Tanre (1992). Atmospherically resistant vegetation index (ARVI) for EOS-MODIS. IEEE Trans. Geosci. Remote Sens. 30(2): 261-270. https://doi.org/10.1109/36.134076

Lacerda, L.N., J.L. Snider, Y. Cohen, V. Liakos, S. Gobbo and G. Vellidis (2022). Using UAV-based thermal imagery to detect crop water status variability in cotton. Smart Agric. Technol. 2: 100029. https://doi.org/10.1016/j.atech.2021.100029

Maimaitijiang, M., V. Sagan, P. Sidike, A.M. Daloye, H. Erkbol and F.B. Fritschi (2020). Crop monitoring using satellite/UAV data fusion and machine learning. Remote Sens. 12(9): 1357. https://doi.org/10.3390/rs12091357

Marang, I.J., P. Filippi, T.B. Weaver, B.J. Evans, B.M. Whelan, T.F.A. Bishop, M.O.F. Murad, D. Al-Shammari and G. Roth (2021). Machine learning optimised hyperspectral remote sensing retrieves cotton nitrogen status. Remote Sens. 13(8): 1428. https://doi.org/10.3390/rs13081428

Misra, G., F. Cawkwell and A. Wingler (2020). Status of phenological research using Sentinel-2 data: A review. Remote Sens. 12(17): 2760. https://doi.org/10.3390/rs12172760

Mourad, R., H. Jaafar, M. Anderson and F. Gao (2020). Assessment of leaf area index models using harmonized Landsat and Sentinel-2 surface reflectance data over a semi-arid irrigated landscape. Remote Sens. 12(19): 3121. https://doi.org/10.3390/rs12193121

Oosterhuis, D.M. and J. Jernstedt (1999). Morphology and anatomy of the cotton plant. In Cotton: Origin, History, Technology, and Production. (C. W. Smith & J. T. Cothren (Eds.)), 1st Ed. John Wiley & Sons; New York. 175-206 pp. ISBN: 9780471180456

Pei, S., Y. Dai, Z. Bai, Z. Li, F. Zhang, F. Yin and J. Fan (2024). Improved estimation of canopy water status in cotton using vegetation indices along with textural information from UAV-based multispectral images. Comput. Electron. Agric. 224: 109176. https://doi.org/10.1016/j.compag.2024.109176

Pei, S., H. Zeng, Y. Dai, W. Bai and J. Fan (2023). Nitrogen nutrition diagnosis for cotton under mulched drip irrigation using unmanned aerial vehicle multispectral images. J. Integr. Agric. 22(8): 2536-2552. https://doi.org/10.1016/j.jia.2023.02.027

Penuelas, J., F. Baret and I. Filella (1995). Semi-empirical indices to assess carotenoids/chlorophyll a ratio from leaf spectral reflectance. Photosynthetica 31(2): 221-230. ISSN (Print): 0300-3604 ISSN (Online): 1573-9058

Pinder, J.E. III and K.W. McLeod (1999). Indications of relative drought stress in longleaf pine from Thematic Mapper data. Photogramm. Eng. Remote Sens. 65(4): 495-501. ISSN (Print): 0099-1112 ISSN (Online): 2575-150X

Pradhan, S., V.K. Sehgal, K.K. Bandyopadhyay, R.N. Sahoo, P. Panigrahi, C.M. Parihar and S.L. Jat (2018). Comparison of vegetation indices from two ground based sensors. J. Indian Soc. Remote Sens. 46(2): 321-326. https://doi.org/10.1007/s12524-017-0671-0

Qi, J., A. Chehbouni, A.R. Huete, Y.H. Kerr and S. Sorooshian (1994). A modified soil adjusted vegetation index. Remote Sens. Environ. 48(2): 119-126. https://doi.org/10.1016/0034-4257(94)90134-1

Radočaj, D., A. Šiljeg, R. Marinović and M. Jurišić (2023). State of major vegetation indices in precision agriculture studies indexed in Web of Science: A review. Agriculture 13(3): 707. https://doi.org/10.3390/agriculture13030707

Rehman, M., A. Bakhsh, M. Zubair, M.I.A. Rehmani, A. Shahzad, S. Nayab, M. Khan, W. Anum, R. Akhtar, N. Kanwal, N. Manzoor and I. Ali (2021). Effects of water stress on cotton (Gossypium spp.) plants and productivity. Egypt. J. Agron. 43(3): 307-315. https://doi.org/10.21608/agro.2021.89343.1272

Ren, Y., Y. Meng, W. Huang, H. Ye, Y. Han, W. Kong and Y. Geng (2020). Novel vegetation indices for cotton boll opening status estimation using Sentinel-2 data. Remote Sens. 12(11): 1712. https://doi.org/10.3390/rs12111712

Rondeaux, G., M. Steven and F. Baret (1996). Optimization of soil-adjusted vegetation indices. Remote Sens. Environ. 55(2): 95-107. https://doi.org/10.1016/0034-4257(95)00186-7

Sapkota, B.R., C.B. Adams, Q. Su and S. Ale (2024). Remote detection of water stress in cotton using a center pivot irrigation system-mounted sensor package. Sci. Rep. 14(1): 23436. https://doi.org/10.1038/s41598-024-74092-2

Shanmugapriya, P., K. Latha, S. Pazhanivelan, R. Kumaraperumal, G. Karthikeyan and N.S. Sudarmanian (2023). Spatial prediction of leaf chlorophyll content in cotton crop using drone-derived spectral indices. Curr. Sci. 123: 1473-1480. https://doi.org/10.18520/cs/v123/i12/1473-1480

Sishodia, R.P., R.L. Ray and S.K. Singh (2020). Applications of remote sensing in precision agriculture: A review. Remote Sens. 12(19): 3136. https://doi.org/10.3390/rs12193136

Sun, Q., Q. Jiao, X. Qian, L. Liu, X. Liu and H. Dai (2021). Improving the retrieval of crop canopy chlorophyll content using vegetation index combinations. Remote Sens. 13(3): 470. https://doi.org/10.3390/rs13030470

Tian, Y., Y. Shuai, C. Shao, H. Wu, L. Fan, Y. Li, X. Chen, A. Narimanov, R. Usmanov and S. Baboeva (2023). Extraction of cotton information with optimized phenology-based features from Sentinel-2 images. Remote Sens. 15(8): 1988. https://doi.org/10.3390/rs15081988

Vidican, R., A. Malinas, O. Ranta, C. Moldovan, O. Marian, A. Ghețe and F. Popovici (2023). Using remote sensing vegetation indices for the discrimination and monitoring of agricultural crops: A critical review. Agronomy 13(12): 3040. https://doi.org/10.3390/agronomy13123040

Wang, Y., C. Xiao, Y. Wang, K. Li, K. Yu, J. Geng and Z. Li (2023). Monitoring of cotton boll opening rate based on UAV multispectral data. Remote Sens. 16(1): 132. https://doi.org/10.3390/rs16010132

Wen, Y., B. Guo, W. Zang, D. Ge, W. Luo and H. Zhao (2020). Desertification detection model in Naiman Banner based on the albedo-modified soil adjusted vegetation index feature space using the Landsat8 OLI images. Geomat. Nat. Hazards Risk 11(1): 544-558. https://doi.org/10.1080/19475705.2020.1734100

Yang, S., R. Wang, J. Zheng, W. Han, J. Lu, P. Zhao, X. Mao and H. Fan (2024). Remote sensing-based monitoring of cotton growth and its response to meteorological factors. Sustainability 16(10): 3992. https://doi.org/10.3390/su16103992

Zeng, Y., D. Hao, A. Huete, B. Dechant, J. Berry, J.M. Chen, J. Joiner, C. Frankenberg, B. Bond-Lamberty, Y. Ryu, J. Xiao, G.R. Asrar and M. Chen (2022). Optical vegetation indices for monitoring terrestrial ecosystems globally. Nat. Rev. Earth Environ. 3(7): 477-493. https://doi.org/10.1038/s43017-022-00298-5